



Received on 08 September 2018; received in revised form 16 November 2018; accepted, 20 November 2018; published 01 May 2019

SPECTROPHOTOMETRIC DETERMINATION OF MEBENDAZOLE THROUGH CHARGE TRANSFER INTERACTIONS

Reem M. Alghanmi* and Lamyaa Yousef Alhazmi

Department of Chemistry, Faculty of Science, University of Jeddah, Jeddah, Saudi Arabia.

Keywords:

Mebendazole,
Charge transfer,
Chloranilic acid, Picric acid,
Determination, Pharmaceutical

Correspondence to Author:

Reem M. Alghanmi

Department of Chemistry,
Faculty of Science, University of
Jeddah, Jeddah, Saudi Arabia.

E-mail: rmalghanmi2018@gmail.com

ABSTRACT: This article presents the development of a direct, simple and sensitive spectrophotometric method for the quantitative analysis of mebendazole (MBz), an anthelmintic medication in its pure and pharmaceutical forms. The method is based on the charge transfer (CT) interactions between MBz, an electron donor, and chloranilic acid (CA), 3,5-dinitrosalicylic acid (DNSA), and picric acid (PA), (all of which are π -acceptors). The products of the CT reactions exhibit new absorption bands at 409 and 310 nm for CA and DNSA in methanol, respectively, and at 402 nm for PA in dichloroethane. Following the optimization of the experimental conditions, linearity ranges for MBz concentrations of 2.00-120, 1.00-40.0 and 2.00-25.0 $\mu\text{g mL}^{-1}$ were achieved for CA-MBz, DNSA-MBz, and PA-MBz, respectively. Furthermore, the limits of detection (LOD) and quantification (LOQ) were calculated. The method was used to determine the MBz concentrations of tablets with good accuracy and precision and without interference from common tablet excipients.

INTRODUCTION: Mebendazole (MBz), *i.e.*, methyl [5- benzol- 1H- benzoimidazole- 2- yl] carbamate **Scheme 1**, is a broad spectrum anthelmintic drug widely used against hookworm, pinworm, roundworm, tapeworm, threadworm and mixed infestations. Furthermore, MBz is widely used against gastrointestinal helminths in both humans and animals^{1, 2}. The most common global diseases are helminthic, and they cause a variety of serious health problems and impact child growth by causing anemia and other nutritional deficiencies³. Thus, the World Health Organization (WHO) categorize MBz as an essential medicine in its capacity as a single-dose treatment for helminthic infections⁴.

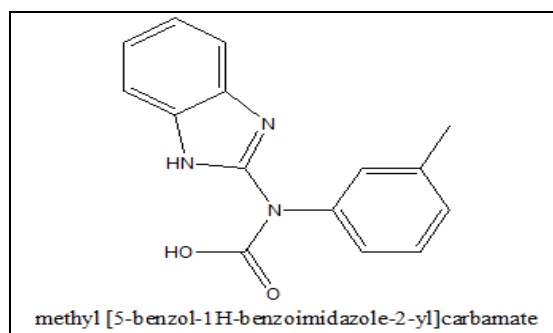
MBz has been shown to exhibit clinical efficiency, minimal side effects, and proven safety. It is available in tablet and syrup form, and its dosage varies for adults and children depending on the worm type being treated⁵.

Several analytical methods have been reported for the determination of MBz in pharmaceutical formulations and biological samples. These methods include the following: titrimetry⁶⁻⁹, UV-visible spectrophotometry^{8, 10-13}, phosphorescence¹⁴, FT-IR spectroscopy¹⁵, proton nuclear magnetic resonance spectrometry¹⁶, fluorimetry^{17, 18}, thermogravimetry¹⁹, membrane-sensor based potentiometry²⁰, polarography²¹⁻²³, voltammetry²⁴, high-performance liquid chromatography²⁵⁻³¹, and high performance thin layer chromatography^{32, 33}. However, many of the above methods suffer from disadvantages such as poor sensitivity, the need for high-cost solvents and reagents, elaborate sample extraction and treatment procedures, heating or cooling steps, and complicated instruments or experimental setups.

<p>QUICK RESPONSE CODE</p> 	<p>DOI: 10.13040/IJPSR.0975-8232.10(5).2504-15</p> <hr/> <p>The article can be accessed online on www.ijpsr.com</p> <hr/> <p>DOI link: http://dx.doi.org/10.13040/IJPSR.0975-8232.10(5).2504-15</p>
-----------------------------------------------------------------------------------------------------------------------	------------------------------------------------------------------------------------------------------------------------------------------------------------------------------------------------------------------------------------------------------------------------------------------------------------------------------

Many drugs can act as electron donors because they contain atoms such as nitrogen, oxygen or sulfur that can donate electrons. Thus, charge transfer (CT) interactions have attracted considerable researchers attention as a means to study drug-receptor interactions, investigate drug action mechanisms and analyze and determine drugs in their pure and pharmaceutical forms and biological samples³⁴.

Accordingly, this study aimed to develop a direct, simple, sensitive and precise spectrophotometric method to detect and quantify MBz in its pure and dosage forms. The method is based on the formation of CT complexes between MBz, an electron donor and chloranilic acid (CA), 3,5-dinitrosalicylic acid (DNSA), and picric acid (PA), all of which are π -acceptors. To the best of the authors' knowledge, this represents the first time this methodology has been applied to the determination of MBz.



SCHEME 1: THE MOLECULAR STRUCTURE OF MEBENDAZOLE, MBz.

MATERIALS AND METHODS: Pure analytical grade mebendazole powder, (MBz, purity $\geq 98\%$) was obtained from Sigma-Aldrich. The pharmaceutical form of MBz (Vermox tablets, 100 mg MBz per tablet from Johnson & Johnson Consumer NV/SA) was obtained from a local pharmacy. CA, DNSA and PA (purities $\geq 98\%$) were obtained from Sigma-Aldrich. Standard stock solutions of CA (5×10^{-3} mol L⁻¹) and DNSA (5×10^{-4} mol L⁻¹) were prepared in methanol and a standard stock solution of PA (1×10^{-3} mol L⁻¹) was prepared in dichloroethane. All reagent solutions were stored in the dark and found to be stable for at least one week. The solvents used throughout the study were obtained from Fisher Scientific at spectroscopic grade and used without further purification.

A standard stock solution of MBz ($1000 \mu\text{g mL}^{-1}$) was prepared by dissolving 100 mg of the pure drug in 15 mL of DMSO and then diluting to 100 mL with methanol. This solution was used for complexation with CA and DNSA. Another standard stock solution of MBz ($1000 \mu\text{g mL}^{-1}$) was prepared for complexation with PA in the same way but using dichloroethane instead of methanol as a solvent. The MBz stock solutions were stored in a refrigerator and found to be stable for at least one week. Working solutions ($200 \mu\text{g mL}^{-1}$) were prepared immediately before measurement by further diluting the stock solution with methanol or dichloromethane. All electronic absorption spectra were measured over the wavelength range 200-700 nm using a UV 1800 (Shimadzu, Japan) UV-Vis instrument connected to a TCC-ZUOA (Shimadzu, Japan) temperature controller unit.

General Procedures (Calibration curves):

CA Acceptor: Aliquots of the working MBz solution with volumes calculated to provide final concentrations in the range 2.00 - $160 \mu\text{g mL}^{-1}$ were transferred into a series of 10-mL calibration flasks. Then, 1 mL of $5 \times 10^{-3} \mu\text{g mL}^{-1}$ CA solution was added to each flask, and the resultant CA-MBz mixtures were diluted to the flask mark with methanol. The absorbances of all of the solutions were recorded at 530 nm against a CA blank.

DNSA Acceptor: Aliquots of the working MBz solution with volumes calculated to provide final concentrations in the range 1.00 - $50.0 \mu\text{g mL}^{-1}$ were transferred into a series of 10-mL calibration flasks. Then, 0.1 mL of $5 \times 10^{-4} \mu\text{g mL}^{-1}$ DNSA solution was added to each flask, and the resultant DNSA-MBz mixtures were diluted to the flask mark with methanol. The absorbances of all of the solutions were recorded at 310 nm against a DNSA blank.

PA Acceptor: Aliquots of the working MBz solution with volumes calculated to provide final concentrations in the range 1.00 - $30.0 \mu\text{g mL}^{-1}$ were transferred into a series of 10-mL calibration flasks. Then, 1 mL of a $1 \times 10^{-3} \mu\text{g mL}^{-1}$ PA solution was added to each flask, and the resultant PA-MBz mixtures were diluted to the flask mark with dichloroethane. The absorbances of all of the solutions were recorded at 402 nm against a PA blank.

In each of the above cases, the absorbance values of all of the solutions were plotted as a function of the MBz concentration to construct calibration curves.

Pharmaceutical Samples Preparation: Ten tablets of the pharmaceutical drug were weighed, ground into powder, and thoroughly mixed. An accurately weighed portion of the powder equivalent to 150 mg of MBz was dissolved in 7.5 mL of DMSO and stirred with gentle warming for 10 min. The solution was filtered, and the first 10 mL was discarded. The remainder was diluted to 50-mL with methanol (for CA and DNSA) or dichloroethane (for PA) to obtain a final concentration of $1000 \mu\text{g mL}^{-1}$. Aliquots of this solution were used to test the suggested method.

RESULTS AND DISCUSSION:

Electronic Spectra: MBz has many electron dense sites and can act as a strong electron donor. Accordingly, the detection of MBz by our spectrophotometric method depends on the reaction expected of MBz with CA, DNSA, or PA to form stable CT complexes.

When using CA as the acceptor, a stable deep purple product is immediately formed upon mixing the MBz and CA solutions in methanol at room temperature. This is accompanied by the appearance of a new absorption band in the electronic spectra at $\lambda_{\text{max}} = 530 \text{ nm}$, which is not observed in the spectra of the free reactants **Fig. 1**.

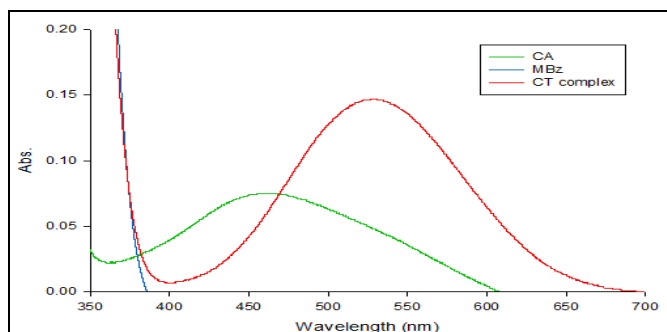
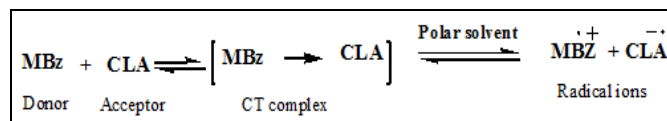


FIG. 1: ELECTRONIC SPECTRA OF CA, MBz AND [MBz-CA] COMPLEX IN METHANOL

This new band is attributed to the formation of a CT complex between MBz and CA. Furthermore, the purple color of the product is due to the formation of the radical anion of CA, which is a result of $\pi-\pi^*$ transition from MBz to CA³⁵, as shown in **Scheme 2**. Methanol, a polar solvent,

promotes the complete transfer of electrons from donors to acceptors, resulting in the complete formation of the CA radical anion³⁶.



SCHEME 2: REACTION OF MBz WITH CA

In the case of DNSA, a new absorption band is detected in the electronic spectra of the DNSA-MBz mixture in the 250-350 nm region ($\lambda_{\text{max}} = 310 \text{ nm}$, **Fig. 2**). This new band indicates the formation of a CT complex between MBz and DNSA. DNSA has both carboxyl and hydroxyl groups, which make it a good proton donor. Therefore, we can reason that the electron transfer from MBz to DNSA will be accompanied by proton transfer from the DNSA to the MBz either from the carboxyl group³⁷ or the hydroxyl group³⁸. The charge and proton transfer interactions enhance the bonding between the MBz and DNSA in the resultant complex.

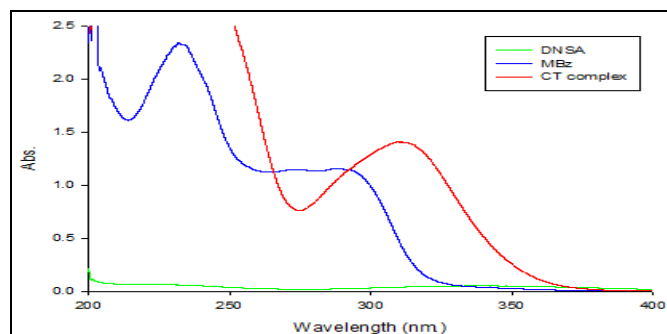
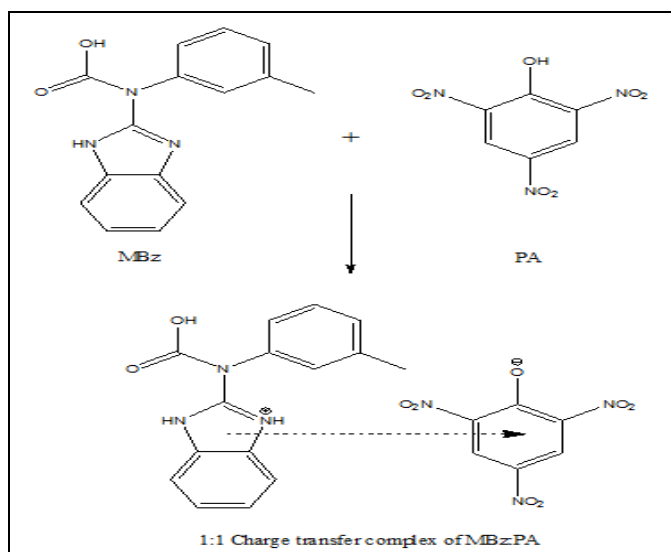


FIG. 2: ELECTRONIC SPECTRA OF DNSA, MBz AND [MBz-DNSA] COMPLEX IN METHANOL

Similarly, a stable intense yellow product is formed when the MBz and PA solutions are mixed in dichloroethane. The electronic absorption spectra of MBz, PA and their mixture are shown in **Fig. 3**, demonstrating the appearance of a new CT band at $\lambda_{\text{max}} = 402 \text{ nm}$. The PA dichloroethane solution is colorless and becomes yellow upon the addition of MBz. The yellow color is due to the formation of picrate ions (phenolate ions)³⁹, which shows that PA does not dissociate in dichloroethane alone but functions as a proton donor in the presence of MBz.

Additionally, several previous studies have concluded that complexation between electron-rich compounds and PA occurs through intermolecular hydrogen bonding⁴⁰⁻⁴².

Thus, a possible mechanism for the reaction between MBz and PA, where a proton transfer from the hydroxyl group of PA to the nitrogen atom in the benzimidazole ring of MBz, is shown in **Scheme 3**. The λ_{\max} values of the CT bands, *i.e.*, 530 nm for CA, 310 nm for DNSA, and 402 nm for PA, were used in all further measurements to ensure the highest sensitivity for the proposed method. The spectrum of the CT complex was measured and compared to that of the blank acceptor solution to eliminate any overlap between the complex and acceptor bands.



SCHEME 3: REACTION POSSIBLE MECHANISM OF MBz WITH PA IN DICHLOROETHANE

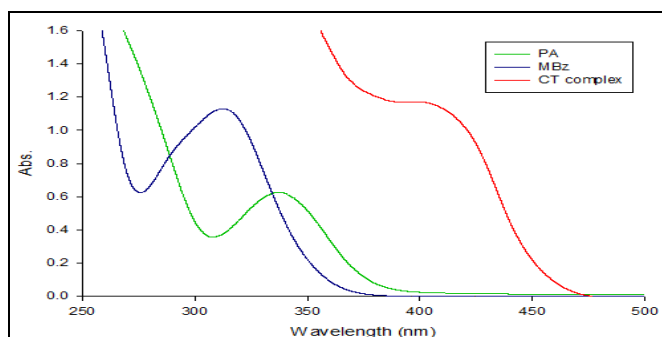


FIG. 3: ELECTRONIC SPECTRA OF PA, MBz AND [MBz-PA] COMPLEX IN DICHLOROETHANE

Optimization of the CT Reaction Conditions:

Effect of the Solvent: The formation of a CT complex between an electron donor and π acceptors can be influenced by the nature of the solvent. Thus, the first parameter studied to optimize the reaction conditions were solvent nature. The absorbance characteristics of the CT complexes were examined in various solvents including acetonitrile, methanol, ethanol, dichloroethane, dichloromethane, and chloroform.

The absorbance values of the CT complexes with CA, DNSA and PA acceptors in different solvents are shown in **Fig. 4**. For CA and DNSA, methanol is the best solvent because stable complexes with the highest absorbances are formed. For PA, the maximum intensity is obtained when dichloroethane is used as the solvent.

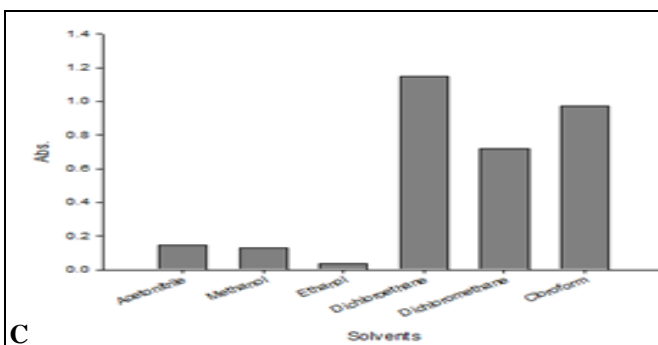
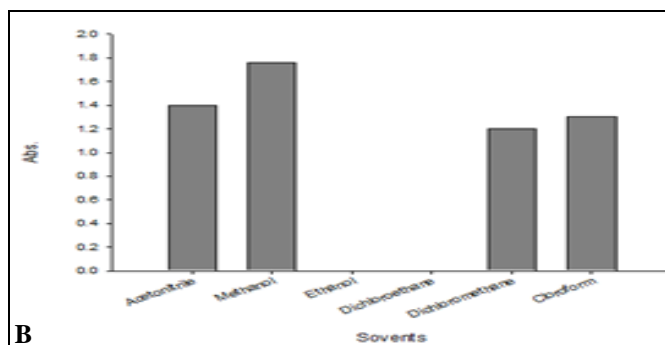
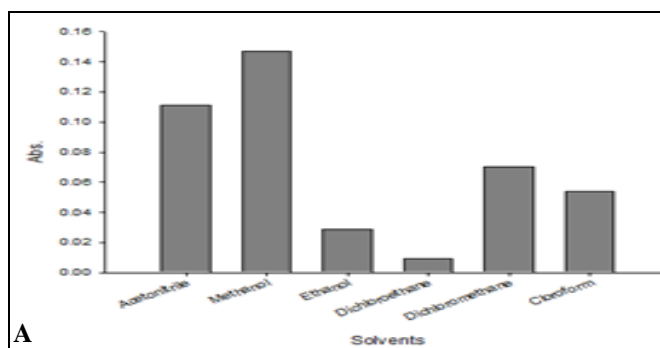


FIG. 4: EFFECT OF SOLVENT ON THE FORMATION OF MBz CT COMPLEXES WITH A-CA, B-DNSA, C-PA

Effect of Acceptor Concentration: The effect of acceptor concentration on the absorbance intensities at the chosen λ_{\max} values was investigated. The absorbances of the CT complexes with different volumes of the acceptor, *i.e.*, CA (5×10^{-3} mol L⁻¹), DNSA (5×10^{-4} mol L⁻¹), and PA (1×10^{-3} mol L⁻¹) were measured. As shown in Fig. 5, the absorbances of the complexes increase as the acceptor volume increases, and the highest absorbances for the complexes are obtained using 1 mL of CA or PA, and 0.1 mL of DNSA in 10 mL calibration flasks.

Effect of the Reaction Time: The effect of the reaction time on the formation of the CT complexes was studied by monitoring the absorbances of the colored products from the reactions between MBz and the acceptors at different times and room temperature.

The CT products exhibit maximum absorbance immediately upon mixing of the MBz and acceptor solutions. Furthermore, the CT products are stable for at least 1 h in the case of CA, and for 2 h in the case of DNSA and PA. Thus, the absorbance values were measured after 1 min in all acceptor-MBz systems to ensure the precision of the measurements.

Effect of Temperature: The effect of temperature on the stability of the formed CT complexes was investigated by measuring the absorbances of mixtures of 5×10^{-4} mol L⁻¹ CA, 5×10^{-6} mol L⁻¹ DNSA, and 1×10^{-4} mol L⁻¹ PA with different concentrations of MBz over the temperature range 20 °C to 40 °C. The experimental results show that the absorbance decreases as the temperature increases and that 20 °C is the optimum temperature for all MBz complexes.

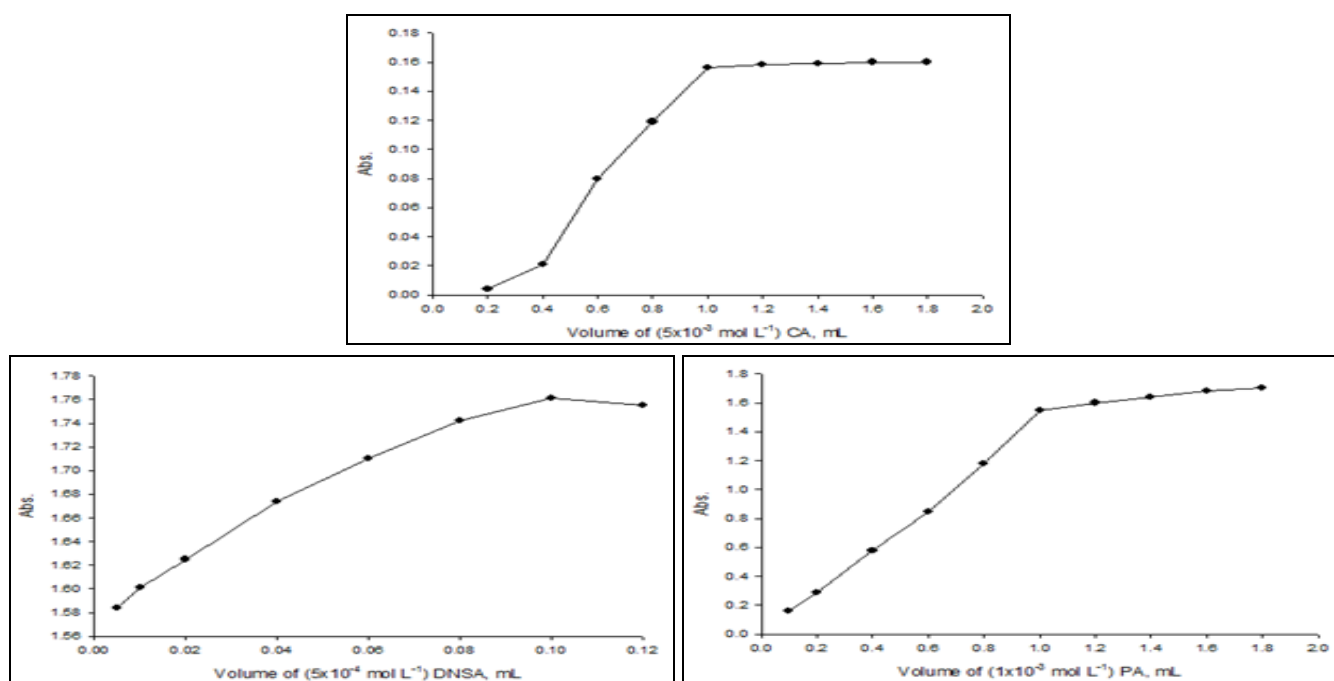


FIG. 5: EFFECT OF ACCEPTOR VOLUME ON THE FORMATION OF MBz CT COMPLEX

Determination of the CT Complex Compositions and the Formation Constants: The molecular composition of the CT complexes that form between MBz and the π acceptors (CA and PA) was estimated using Job's method of continuous variations⁴³. For both complexes, the plot reaches a maximum absorbance at a 0.5-mole fraction, indicating the formation of a 1:1 CT complex Fig. 6. However, the composition of the DNSA complex with MBz was estimated using the Benesi-Hildebrand (BH) equation⁴⁴ and the

straight-line method by measuring the absorbance of the CT complex at different concentrations of MBz. For the BH equation to be applied, one of the two reactants must be present in large excess⁴⁵.

$$\frac{[C_A]}{A} = \frac{1}{K_f \cdot \epsilon} \cdot \frac{1}{[C_D]} + \frac{1}{\epsilon} \quad \dots(1)$$

Where, $[C_A]$ and $[C_D]$ are the initial concentrations of DNSA and MBz respectively, and A is the absorbance of the CT complex at λ_{\max} . By plotting

the values of $[C_A]/A$ against $1/[C_D]$, a straight line is obtained ($r \geq 0.9992$), indicating the formation of a 1:1 CT complex [MBz: DNSA], as shown in **Fig. 7**. The 1:1 ratio for all studied complexes is in agreement with the appearance of only one new absorption band in all spectra **Fig. 1-3**. This ratio could be related to the steric hindrance effect of the MBz molecule⁴⁶. The formation constants, K_f ($L \text{ mol}^{-1}$) and extinction coefficients, ε ($L \text{ mol}^{-1} \text{ cm}^{-1}$), of the CT complexes, were calculated using the absorbance values obtained by adding different MBz concentrations to a certain concentration of CA or PA, and by applying the modified Benesi-Hildebrand equation⁴⁴ for a 1:1 molar ratio **Eq. 2**:

$$C_D^o C_A^o / A = 1 / K_f \varepsilon + (C_D^o + C_A^o) / \varepsilon \dots\dots(2)$$

Where, C_D^o and C_A^o are the concentrations of MBz and the acceptor, respectively, and A is the absorbance of the CT-bands. By plotting the values of $C_D^o C_A^o / A$ against the $C_D^o + C_A^o$ values from **Eq. 2**, linear plots are obtained, confirming the

formation of 1:1 complex **Fig. 8 and 9**. The K_f and ε values were calculated from the plots, where the slope and intercept are equal to $1/\varepsilon$ and $1/K_f \varepsilon$, respectively. Conversely, the K_f and ε values of the DNSA-MBz complex were calculated using the BH equation in the form of **Eq. 1**. The K_f , ε , and λ_{max} values for all of the complexes are compiled in **Table 1**. The K_f values are 2.60×10^3 , 3.33×10^2 and 40.0×10^3 for the [CA-MBz], [DNSA-MBz] and [PA-MBz] CT complexes, respectively.

These high K_f values confirm the high stability of the CT complexes formed. The K_f values reveal that [PA-MBz] complex has the highest value of the formation constant K_f which confirms the high stability of this complex as a result of the expected high accepting nature of PA compared with both CA and DNSA. PA has three strong withdrawing nitro groups in conjugation with an aromatic ring which causes high delocalization leads to a great increase in the acidity of PA⁴⁷.

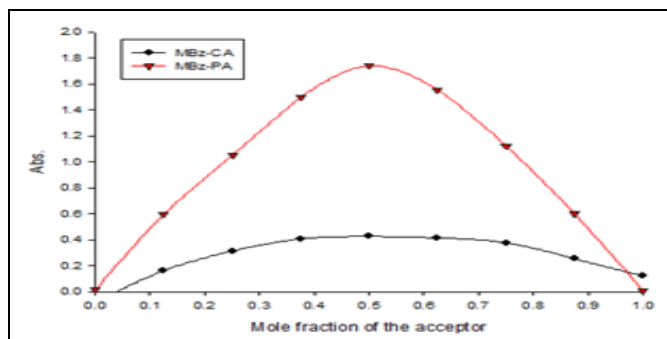


FIG. 6: JOB'S METHOD PLOT FOR MBz CT COMPLEXES WITH CA OR PA

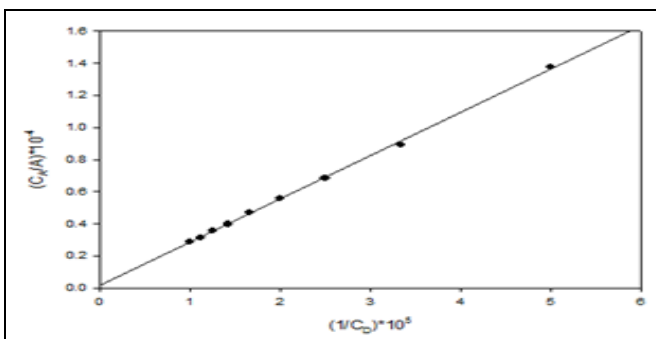


FIG. 7: BENESI-HILDEBRAND PLOT OF [MBz-DNSA] COMPLEX

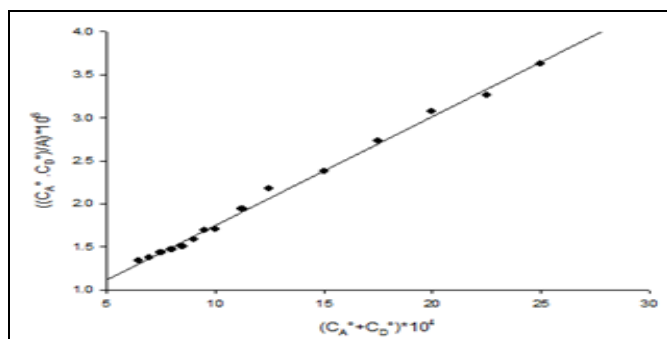


FIG. 8: BENESI-HILDEBRAND PLOT OF [MBz-CA] COMPLEX

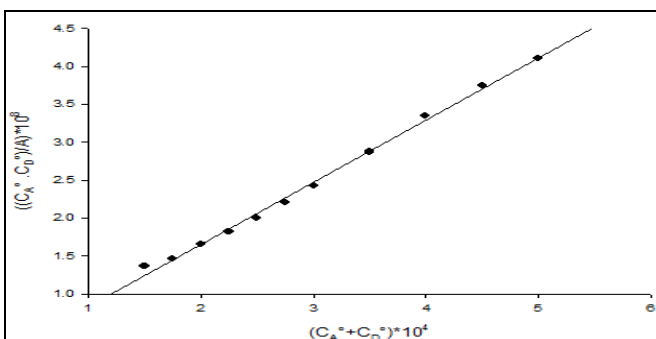


FIG. 9: BENESI-HILDEBRAND PLOT OF [MBz-PA] COMPLEX

Determination of Some Spectroscopic Physical Data: The experimental oscillator strengths (f)⁴⁸ and transition dipole moments (μ)⁴⁹ of the MBz CT complexes were determined by applying the following equations⁵⁰:

$$f = 4.32 \times 10^{-9} [\varepsilon_{max} \cdot \Delta \nu_{1/2}] \dots\dots(3)$$

$$\mu = 0.0958 [\varepsilon_{max} \cdot \Delta \nu_{1/2} / \bar{\nu}_{max}]^{1/2} \dots\dots(4)$$

Where $\Delta\nu_{1/2}$ is the half bandwidth of the absorbance in cm^{-1} , and ε_{max} and $\bar{\nu}_{\text{max}}$ are the molar extinction coefficient and wavenumber for the maximum absorption of the CT complexes, respectively.

Table 1 shows that both the oscillator strength and transition dipole moment values for all complexes are relatively high, which confirms the strong interactions between MBz and the π acceptors. These results are consistent with the lower CT energy values, E_{CT} , which were calculated from **Eq. 5**⁵¹, and are listed in **Table 1**:

$$E_{\text{CT}} = 1243.667 / \lambda_{\text{CT}} \dots\dots(5)$$

Moreover, the ionization potential (I_p) value of the donor, *i.e.*, MBz, was calculated using the following equation⁵²:

$$I_p(\text{eV}) = 5.76 + 1.53 \times 10^{-4} \cdot \bar{\nu}_{\text{max}} \dots\dots(6)$$

Where, $\bar{\nu}_{\text{max}}$ is the wavenumber of the CT band in cm^{-1} . **Table 1** shows the value of I_p . The dissociation energy (W) of the three CT complexes was calculated using the following relationship⁵³:

$$E_{\text{CT}} = I_p - E_A - W \dots\dots(7)$$

TABLE 1: THE SPECTROSCOPIC DATA OF THE CT COMPLEXES

Acceptor	$K_{\text{CT}} \times 10^{-3}$ L mol^{-1}	$\varepsilon \times 10^{-3}$ $\text{L mol}^{-1} \text{cm}^{-1}$	F	μ (Debye)	E_{CT} (eV)	W (eV)	I_p (eV)	R_N (eV)	$-\Delta G^\circ$ kJ mol^{-1}
CA	2.600	0.77	0.090	3.189	2.346	5.201	8.647	0.004	19.50
DNSA	1.000	17.20	30.34	44.70	4.011	6.099	10.70	0.509	14.40
PA	40.00	12.50	10.48	29.92	3.094	5.752	9.566	0.242	26.27

Validation of the Proposed Method: The proposed spectrophotometric method for the determination of MBz is based on the formation of stable CT complexes between MBz and CA or DNSA in methanol, or PA in dichloroethane with a simple 1:1 molecular composition.

The linearity, accuracy, precision, recovery, robustness, and ruggedness of the methods were assessed to validate the proposed method according to the International Conference on Harmonization (ICH) guidelines⁵⁷.

Linearity and Sensitivity: Under the optimized experimental reaction conditions, MBz concentration calibration curves were constructed for all acceptors (CA, DNSA, and PA). The curves are linear over the concentration ranges 2.00-120,

Where, E_A is the electron affinity of the values acceptors, which are 1.1⁵³, 0.59 and 0.72 eV⁵⁴ for CA, DNSA, and PA, respectively. The resonance energy (R_N) values of the CT complexes in the ground state are determined using the Briegleb and Czekalla equation⁵⁵:

$$\varepsilon_{\text{CT}} = 7.7 \times 10^4 / [h\nu_{\text{CT}} / [R_N] - 3.5] \dots\dots(8)$$

Where, ε_{CT} is the molar extinction coefficient of the complexes at the maximum absorbance value of the CT band, ν_{CT} is the frequency of the CT band, and R_N is the resonance energy of the complex, which is a parameter of the ground state property. The W and R_N values are given in **Table 1**.

Finally, the standard free energy changes for complexation, ΔG° (kJ mol^{-1}) were estimated from the K_f values at 20 °C using the equation⁵⁶:

$$\Delta G^\circ = -2.303RT \log K_f \dots\dots(9)$$

Where, R is the gas constant ($8.314 \text{ J mol}^{-1} \text{ K}$). The negative values of ΔG° listed in **Table 1** indicate that the complexation processes between MBz and CA, DNSA or PA are exothermic and simultaneous.

1.00-40.0, and 1.00-25.0 $\mu\text{g mL}^{-1}$ for CA, DNSA, and PA, respectively. The regression equations of the lines were derived using the least square method⁵⁸. The limits of detection (LOD) and limit of quantification (LOQ) were calculated using the following equations according to the IUPAC definition⁵⁹:

$$\text{LOD} = 3.3S_a/b \dots\dots(10)$$

$$\text{LOQ} = 10S_a/b \dots\dots(11)$$

Where S_a is the standard deviation of the intercept and b is the slope of the calibration curve. The linear range, LOD, LOQ, intercept a slope b , S_a , the standard deviation of the slope (S_b), the standard deviation of residuals ($S_{y/x}$), and correlation coefficient (R) values are shown in **Table 2**.

The small $S_{y/x}$ values indicate that the points are close to a straight line. Additionally, the small intercept values of the regression equation and the excellent correlation coefficient values ($R > 0.9986$) confirm the classic linear relationship between the MBz concentration and the absorbance values in

the proposed methods. Moreover, the LOD and LOQ values in **Table 2** indicate that the method utilizing complexation with DNSA is more sensitive for MBz determination than that with the other acceptors (CA or PA).

TABLE 2: LINEARITY, REGRESSION EQUATION AND SENSITIVITY PARAMETERS OF THE PROPOSED METHODS (N = 7)

Parameter	Acceptor		
	CA	DNSA	PA
Wavelength (λ_{max}), nm	530	310	402
Linear range, $\mu\text{g mL}^{-1}$	2.00-120.0	1.00-40.0	2.00-25.00
Molar absorptivity (ϵ), $\text{L mol}^{-1} \text{cm}^{-1}$	770	17200	12500
Limit of detection (LOD), $\mu\text{g mL}^{-1}$	3.129	0.931	1.307
Limit of quantification (LOQ), $\mu\text{g mL}^{-1}$	9.483	3.104	3.959
Regression equation ^a			
Intercept, $a \pm S_a$	$0.0068 \pm 1.00 \times 10^{-3}$	$0.0081 \pm 5.4 \times 10^{-3}$	$0.021 \pm 8.721 \times 10^{-3}$
Slope, $b \pm S_b$	$0.0011 \pm 1.48 \times 10^{-5}$	$0.0494 \pm 0.3 \times 10^{-3}$	$0.022 \pm 0.576 \times 10^{-3}$
$S_{y/x}$	1.70×10^{-3}	1.53×10^{-2}	1.17×10^{-2}
Correlation coefficient, R	0.9994	0.9996	0.9986
Stability of colored products (h)	1	2	2

^a $A = a + bC$, where A is the absorbance, C is the MBz concentration in ($\mu\text{g mL}^{-1}$), a is the intercept and b is the slope

Accuracy and Precision: The accuracy and precision of the MBz determination method were established by analyzing solutions of four or five different pure MBz concentrations (within the linear range). The measurements were replicated five times during the day (intra-day) and over three consecutive days (inter-day) using the proposed method. The relative standard deviation, (% RSD), relative error (% RE) and percent recovery were calculated, and the results are summarized in **Table 3**. The relative standard deviation values for CA (% RSD $\leq 1.67\%$ for intra-day; % RSD $\leq 2.00\%$ for

inter-day), DNSA (% RSD $\leq 0.47\%$ for intra-day; % RSD $\leq 0.54\%$ for inter-day), and PA (% RSD $\leq 0.95\%$ for intra-day; % RSD $\leq 1.18\%$ for inter-day) are low, confirming the high precision of the proposed method. Also, the small % RE values shown in **Table 3** indicate the good accuracy of the method for the determination of MBz with all three acceptors. Moreover, the intra-day and inter-day precision and accuracy results indicate the excellent repeatability and reproducibility of the proposed method.

TABLE 3: EVALUATION OF INTRA-DAY AND INTER-DAY ACCURACY AND PRECISION

Acceptor	MBz taken, $\mu\text{g mL}^{-1}$	Intra-day ($n = 5$)			Inter-day ($n = 3$)				
		Found, $\mu\text{g mL}^{-1}$ \pm Confidence limits ^a	% Recovery	% RSD ^b	% RE ^c	Found, $\mu\text{g mL}^{-1}$ \pm Confidence limits ^a	% Recovery	% RSD ^a	% RE ^b
CA	30	29.82 \pm 0.62	99.39	1.67	0.61	29.45 \pm 0.78	98.18	1.07	1.82
	50	49.64 \pm 0.62	99.27	1.00	0.73	49.27 \pm 2.26	98.55	1.85	1.45
	70	69.64 \pm 0.62	99.48	0.72	0.52	69.58 \pm 3.45	99.39	2.00	1.61
	90	89.10 \pm 1.24	98.99	1.12	1.01	89.58 \pm 3.45	99.53	1.55	0.47
	110	108.9 \pm 1.89	99.01	1.40	0.99	109.15 \pm 2.32	99.23	0.85	0.77
DNSA	8	7.982 \pm 0.03	99.77	0.34	0.22	8.060 \pm 0.07	100.8	0.34	0.79
	15	15.05 \pm 0.05	100.3	0.24	0.31	15.09 \pm 0.10	100.6	0.26	0.62
	18	17.97 \pm 0.11	99.85	0.48	0.15	18.20 \pm 0.21	101.1	0.47	1.10
	25	25.08 \pm 0.06	100.3	0.20	0.32	25.09 \pm 0.10	100.4	0.16	0.37
PA	6	5.95 \pm 0.02	99.17	0.34	0.83	5.94 \pm 0.12	99.02	0.77	0.98
	8	7.97 \pm 0.04	99.61	0.52	0.87	7.91 \pm 0.24	99.64	1.18	0.36
	12	11.88 \pm 0.08	98.98	0.64	1.02	11.93 \pm 0.24	99.38	0.79	0.62
	17	16.82 \pm 0.17	98.95	0.95	1.04	16.96 \pm 0.28	99.74	0.67	0.26
	23	22.80 \pm 0.13	99.15	0.55	0.85	22.87 \pm 0.40	99.41	0.70	0.59

^a Average $\pm \frac{t_{0.05}SD}{\sqrt{n}}$, at 95% confidence level, ^b %RSD, relative standard deviation; ^c % RE, relative error

Robustness: The robustness of the method was investigated by making minor changes to two experimental variables, *i.e.*, the acceptor volume (± 0.1 mL) and reaction time (± 0.5 min), for three different concentrations of pure MBz. The recovery percentage and % RSD values were calculated, and

the results are given in **Table 4**. The recovery percentage and % RSD values indicate that small variations in the variables do not significantly affect the results of the proposed method, confirming the robustness of the proposed method for the determination of MBz.

TABLE 4: ROBUSTNESS OF THE PROPOSED METHODS

Acceptor	Parameter	MBz taken, $\mu\text{g mL}^{-1}$	Found, $\mu\text{g mL}^{-1} \pm \text{SD}$	% Recovery	% RSD	
CA (n = 5)	Volume of 5×10^{-4} mol L ⁻¹ CA (1.00 ± 0.10 mL)	50	49.73 \pm 0.45	99.45	0.91	
		70	69.82 \pm 0.81	99.74	1.16	
		90	89.09 \pm 0.76	98.99	0.85	
	Reaction time (1.00 ± 0.30 min)	50	50.09 \pm 0.67	100.2	0.91	
		70	70.09 \pm 0.67	100.1	1.16	
		90	89.45 \pm 0.76	99.39	0.85	
	DNSA (n = 5)	Volume of 5×10^{-4} mol L ⁻¹ DNSA (0.1 ± 0.02 mL)	8.0	7.997 \pm 0.03	99.96	0.32
			15	15.01 \pm 0.05	100.1	0.32
			25	24.97 \pm 0.08	99.87	0.35
Reaction time (1.00 ± 0.30 min)		8.0	8.051 \pm 0.03	100.9	0.41	
		15	15.15 \pm 0.09	101.0	0.62	
		25	25.25 \pm 0.11	101.0	0.44	
PA (n = 7)	Volume of 1×10^{-4} mol L ⁻¹ PA (1.00 ± 0.10 mL)	10	9.91 \pm 0.04	99.08	0.44	
		15	14.85 \pm 0.16	99.00	1.10	
		20	20.06 \pm 0.13	100.3	0.64	
	Reaction time (1.00 ± 0.30 min)	10	9.950 \pm 0.08	99.54	0.78	
		15	15.03 \pm 0.09	100.2	0.60	
		20	20.11 \pm 0.19	100.5	0.96	

Ruggedness: The ruggedness of the method was evaluated using the proposed method to determine the MBz concentration under the same experimental conditions on two different

instruments and with two different analysts. The results are shown in **Table 5** and indicate the reproducibility of the proposed method as the % RSD does not exceed 2%.

TABLE 5: RUGGEDNESS OF THE PROPOSED METHODS

Acceptor	Parameter	MBz taken, $\mu\text{g mL}^{-1}$	Found, $\mu\text{g mL}^{-1} \pm \text{SD}$	% Recovery	% RSD
CA (n = 5)	Analyst I	50	49.64 \pm 0.50	99.27	1.00
		70	69.82 \pm 0.50	99.74	0.71
	Analyst II	50	50.36 \pm 0.76	100.7	1.51
		70	70.18 \pm 0.26	100.3	0.91
	Instrument I	50	49.64 \pm 0.50	99.27	1.00
		70	69.82 \pm 0.50	99.74	0.71
DNSA (n = 5)	Instrument II	50	50.18 \pm 1.11	100.3	2.22
		70	70.36 \pm 0.76	100.3	1.08
	Analyst I	15	15.03 \pm 0.09	100.2	0.59
		25	25.02 \pm 0.33	100.1	1.35
	Analyst II	15	15.39 \pm 0.11	102.6	0.73
		25	25.05 \pm 0.33	100.2	0.34
PA (n = 5)	Instrument I	15	15.03 \pm 0.09	100.2	0.59
		25	25.02 \pm 0.33	100.1	1.35
	Instrument II	15	14.79 \pm 0.09	98.64	0.63
		25	25.05 \pm 0.06	100.2	0.22
	Analyst I	10	10.05 \pm 0.09	100.5	0.88
		15	15.00 \pm 0.10	100.0	0.70
PA (n = 5)	Analyst II	10	9.98 \pm 0.12	99.77	1.18
		15	14.72 \pm 0.21	98.15	1.42
	Instrument I	10	10.05 \pm 0.09	100.5	0.88
		15	15.00 \pm 0.10	100.0	0.70
	Instrument II	10	9.99 \pm 0.10	99.95	0.98
		15	15.02 \pm 0.06	100.1	0.39

Recovery Study: Method validity was confirmed through a recovery study. The recovery was estimated using a standard addition method by adding three different concentration levels of pure MBz to the commercial form of the drug (Vermox® tablets). The total MBz concentration was determined using the proposed method using the different acceptors (CA, DNSA, and PA). The recovery percentage values in **Table 6** show that all three acceptors afford good accuracies, and the

recovery percentage values range from 99.19% to 99.54%, 99.09% to 100.2%, and 98.77% to 100.1% for CA, DNSA, and PA, respectively. Furthermore, the % RSD values range from 0.76% to 1.02%, 0.13% to 0.34%, and 0.47% to 1.15% for CA, DNSA, and PA, respectively. Also, these results indicate that the co-formulated substances and common excipients do not interfere with the determination of MBz concentration.

TABLE 6: RESULTS OF RECOVERY STUDY FOR TABLETS

Acceptor	MBz in tablet, $\mu\text{g mL}^{-1}$	Pure MBz added, $\mu\text{g mL}^{-1}$	Total found, $\mu\text{g mL}^{-1} \pm \text{SD}$	% Recovery	% RSD
CA (n = 5)	60.00	20.00	79.64 \pm 0.81	99.54	1.02
	60.00	30.00	89.27 \pm 0.91	99.19	1.01
	60.00	40.00	99.45 \pm 0.76	99.45	0.76
DNSA (n = 5)	15.00	5.000	19.98 \pm 0.04	99.89	0.19
	15.00	10.00	25.05 \pm 0.03	100.2	0.13
	15.00	15.00	29.73 \pm 0.10	99.09	0.34
PA (n = 5)	5.00	5.00	9.88 \pm 0.11	98.77	1.15
	5.00	10.00	14.99 \pm 0.10	99.97	0.69
	5.00	15.00	20.01 \pm 0.09	100.1	0.47

Analysis of the Pharmaceutical Forms: The proposed method was applied to determine the MBz concentration in Vermox® tablets. The analysis results are reported as the recovery percentage \pm standard deviation **Table 7**. The obtained results were statistically compared with

those obtained using the reference method⁶ by the Student's *t*-test and *F*-test for accuracy and precision, respectively, at a 95% confidence level. The *t*-test and *F*-test values in **Table 7** show that there are no significant differences between the proposed method and the reference method.

TABLE 7: DETERMINATION OF MBz IN VERMOX® TABLETS USING CA, DNSA, AND PA ACCEPTORS

Acceptor	Taken, $\mu\text{g mL}^{-1}$	Found*, $\mu\text{g mL}^{-1} \pm \text{SD}$		% Recovery		F-test	t-test
		Proposed method	Reference method	Proposed method	Reference method		
CA	40	39.78 \pm 0.47	39.33 \pm 0.30	99.45	98.32	2.486	0.751
DNSA	15	15.05 \pm 0.10	14.78 \pm 0.16	100.3	98.53	2.620	1.820
PA	20	20.05 \pm 0.20	19.73 \pm 0.37	100.2	98.63	3.467	1.087

*Average value of five determinations. The value of *t* (tabulated) at 95% confidence level is 2.306. The value of *F* (tabulated) at 95% confidence level and is 6.388.

CONCLUSION: A direct, simple and accurate method for the determination of pure and pharmaceutical formulations of MBz has been developed. This method is based on monitoring the CT interactions between MBz and CA, DNSA or PA reagents, using a spectrophotometric technique. The formed complexes have stoichiometries of 1:1 in all cases. The excellent correlation coefficient values and small intercept values confirm the good linearity of the MBz calibration curves.

Moreover, the calculated LOD and LOQ values indicate that complexation with DNSA is more sensitive for MBz determination than that with the other acceptors. We can conclude from the

obtained validation results that the proposed method has high accuracy, good repeatability, and excellent reproducibility. Additionally, this method is simple, rapid, and inexpensive and does not require critical reactions or complicated treatments, which are attractive features for analytical pharmaceutical studies.

ACKNOWLEDGEMENT: Nil

CONFLICT OF INTEREST: Nil

REFERENCES:

1. Carke EGC: Isolation and Identification of Drugs. The Pharmaceutical Press, London, Second Edition 1975.

2. Conesa AJ, Pinilla JM and Hernandez L: Determination of mebendazole in urine by cathodic stripping voltammetry. *Analytical Chimica Acta* 1996; 331: 111-16.
3. Awasthi S, Bundy DAP and Savioli L: Helminth infections. *The British Medical Journal* 2003; 327(7412): 431-33.
4. Crompton DW, Montresor A, Nesheim MC and Savioli L: *Controlling Disease Due to Helminth Infections*. Geneva: World Health Organization 2003.
5. Drug Index, New Delhi, Passi Publications 1999; 3: 307.
6. Wahbi AM and Onsy S: Determination of mebendazole. *Talanta* 1978; 25: 716-17.
7. Patel AA, Gandhi TP and Patel VC: Estimation of mebendazole in raw materials and formulations. *Indian Journal of Pharmacology* 1978; 40: 20-21.
8. Mohammed FA, Sidhom MB and Hussein HA: Titrimetric and spectrophotometric determination of mebendazole and flubendazole using N-bromosuccinimide. *Bulletin of Pharmaceutical Science, Assiut University* 1986; 9: 92-04.
9. El-Bardicy MG, Mohammed MY and Tawakkol MS: Determination of mebendazole *via* its iodobismuthate complex. *Bulletin of Faculty of Pharmacy, Cairo University* 1993; 31: 287-90.
10. El-Bardicy MG, Mohammed MY and Tawakkol MS: Spectrophotometric determination of mebendazole. *Bulletin of Faculty of Pharmacy, Cairo University* 1990; 28: 11-14.
11. Swamy N and Basavaiah K: Selective and sensitive assay of mebendazole in pharmaceuticals using bromocresol green by spectrophotometry. *Thai Journal of Pharmaceutical Science* 2013; 37: 171-85.
12. Swamy N, Prashanth KN and Basavaiah K: Spectrophotometric assay of mebendazole in dosage forms using sodium hypochlorite. *Journal of Applied Spectroscopy* 2014; 81: 525-533.
13. Parakh DR, Patil MP, Sonawane SS and Jain CP: Development and validation of a spectrophotometric method for estimation of mebendazole in bulk and pharmaceutical formulation. *World Journal of Pharmaceutical Research* 2015; 4: 2223-2235.
14. Baeyens WRG, Abdel Fattah F and De Moerlosse P: Low-temperature phosphorescence analysis of mebendazole and related imidazoles. *Analytical Letters* 1985; 18: 2105-26.
15. Da Silva VH, Goncalves JL, Vasconcelos FVC, Pimentel MF and Pereira CF: Quantitative analysis of mebendazole polymorphs in pharmaceutical raw materials using near-infrared spectroscopy. *Journal of Pharmaceutical Biomedical Analysis* 2015; 115: 587-93.
16. Al-Khamees HA and El-Shazly BM: Determination of mebendazole and its formulations using ¹H nuclear magnetic resonance spectrometry. *Anal* 1988; 113: 599-02.
17. Abdel-Fattah F, Baeyens W and De-Moerlose P: Fluorimetric determination of mebendazole and flubendazole in pharmaceutical dosage forms after alkaline hydrolysis. *Analytical Chimica Acta* 1983; 154: 351.
18. Baeyens W, Abdel-Fattah F and De-Moerlose P: Fluorimetric analysis of mebendazole and flubendazole with hydrogen peroxide. *Journal of Pharmaceutical and Biomedical Analysis* 1985; 3: 397-04.
19. Gomes APB, Correia LP, Simoes MOS and Macedo RO: Development of a thermogravimetric method to the quantitative determination of mebendazole. *Journal of Thermal Analysis and Calorimetry* 2007; 87: 919-25.
20. Kumar KG, Sareena J, Augustine P, Remalakshmy P and Beena S: Mebendazole selective membrane sensor and its application to pharmaceutical analysis. *Analytical Science* 2007; 23: 291-94.
21. Pinzauti S, La-Porta E and Papeschi G: D.C. Polarography for mebendazole analysis. *Journal of Pharmaceutical and Biomedical Analysis* 1983; 1: 223-28.
22. Temezer A, Ozaltin N, Orbey MT and Ozcan T: Electrochemical reduction of mebendazole and its determination in a pharmaceutical dosage form by differential pulse polarography. *Journal of Pharmacy (Belgium)* 1987; 42: 247-50.
23. Jeyaseelan C and Joshi AP: Study of mebendazole by differential pulse polarography. *International Journal of ChemTech Research* 2009; 1: 596-01.
24. Ghalkhani M and Shahrokhian S: Adsorptive stripping differential pulse voltammetric determination of mebendazole at a graphene nanosheets and carbon nanospheres/chitosan modified glassy carbon electrode. *Sensors and Actuators B: Chemical* 2013; 185: 669-74.
25. Sadana GS and Parikh GG: A high performance liquid chromatographic method for the determination of mebendazole from its pharmaceutical preparations. *Indian Drugs* 1987; 24: 533-34.
26. Argekar AP, Raj SV and Kapadia SU: Simultaneous determination of mebendazole and pyrantel pamoate from tablets by high-performance liquid chromatography-reverse phase (RP-HPLC). *Talanta* 1997; 44: 1959-65.
27. Halkar UP, Rane SH and Bhandari NP: Reverse phase high-performance liquid chromatographic determination of pyrantel pamoate and mebendazole in tablets. *Indian Drugs* 1997; 34: 194-96.
28. Al-Kurdi Z, Al-Jallad T, Badwan A and Jaber AMY: High-performance liquid chromatography method for determination of methyl- 5- benzoyl- 2- benzimidazole carbamate (mebendazole) and its main degradation product in pharmaceutical dosage forms. *Talanta* 1999; 50: 1089-97.
29. Gomes AR and Nagaraju V: High-performance liquid chromatographic separation and determination of the process related impurities of mebendazole, fenbendazole and albendazole in bulk drugs. *Journal of Pharmaceutical and Biomedical Analysis* 2001; 26: 919-27.
30. Ramesh R, Yadgire SK and Bhanu R: Simultaneous determination of levamisole HCL and mebendazole in tablets by reverse phase HPLC. *Indian Drugs* 2001; 38: 67-68.
31. Nubia PK and Marcelo SM: Validation of an analytical methodology for the simultaneous dosing of mebendazole and thiabendazole by high-performance liquid chromatography. *Quimica Nova* 2007; 30: 1359-61.
32. Zarpkar SS, Kolte SS and Rane SH: Simultaneous determination of pyrantel pamoate and mebendazole in tablets by high-performance thin layer chromatography. *Indian Drugs* 1997; 34: 707-09.
33. Anon: Simultaneous determination of pyrantel pamoate and mebendazole in tablets by high-performance thin layer chromatography. *Indian Drugs* 1998; 35: 49-51.
34. Basavaiah K: Determination of some psychotropic phenothiazine drugs by charge-transfer complexation reaction with chloranilic acid. *Il Farmaco* 2010; 59: 315-21.
35. Alghanmi RM and Habeeb MM: Spectral and solvation effect studies on charge transfer complex of 2, 6-diaminopyridine with chloranilic acid. *Journal of Molecular Liquids* 2013; 181: 20-28.
36. Salem H: Analytical study for the charge-transfer complexes of pregabalin. *E-Journal of Chemistry* 2009; 6: 332-40.
37. Singh N, Khan IM, Ahmad A and Javed S: Synthesis, crystallographic and spectrophotometric studies of charge

- transfer complex formed between 2,2'-bipyridine and 3,5-dinitrosalicylic acid. *Journal of Molecular Liquids* 2014; 191: 142-50.
38. Smith G, Lynch DE, Byriel K and Kennard CHL: Molecular cocrystals of carboxylic acids. XX the crystal structures of 3,5-dinitrosalicylic acid and its adducts with the isomeric monoaminobenzoic acids. *Australian Journal of Chemistry* 1995; 48: 1133-49.
39. Higuchi T and Brochmann-Hanssen E: *Pharmaceutical Analysis*, New Delhi, India: CBS Publishers 1997.
40. El-Habeeb AA, Al-Saif FA and Refat MS: Charge-transfer interactions of metoclopramide nausea drug against six kinds of π -acceptors: Spectral and thermal discussions. *Spectrochimica Acta A* 2014; 123: 455-66.
41. Refat MS, Saad HA and Adam AM: Spectral, thermal and kinetic studies of charge-transfer complexes formed between the highly effective antibiotic drug metronidazole and two types of acceptors: σ - and π -acceptors. *Spectrochimica Acta A* 2015; 141: 202-10.
42. Belal TS, El-Kafrawy DS, Mahrous MS, Abdel-Khalek MM and Abo-Gharam AH: Validated spectrophotometric methods for determination of sodium valproate based on charge transfer complexation reactions. *Spectrochimica Acta A* 2016; 155: 47-53.
43. Job P: *Advanced Physicochemical Experimental*, London, UK: Pitman 1964.
44. Benesi HA and Hildebrand JH: A Spectrophotometric investigation of the interaction of iodine with aromatic hydrocarbons. *Journal of the American Chemical Society* 1949; 71: 2703-77.
45. Duymus H, Arslan M, Kucukislamoglu M and Zangin M: Charge transfer complex studies between some non-steroidal anti-inflammatory drugs and π -electron acceptors. *Spectrochimica Acta A* 2006; 65: 1120-24.
46. Refat MS, Ahmed HA, Grabchev I and El-Zayat LA: Spectroscopic and structural characterization of the charge-transfer interaction of N, N'-bis-alkyl derivatives of 1,4,6,8-naphthalenediimide with chloranilic and picric acids. *Spectrochimica Acta A* 2008; 70: 907-15.
47. Gaballa AS and Amin AS: Preparation, spectroscopic and antibacterial studies on charge-transfer complexes of 2-hydroxypyridine with picric acid and 7,7',8,8'-tetracyano-p-quinodimethane. *Spectrochimica Acta A* 2015; 145: 302-12.
48. Leve ABP: *Inorganic Electronic Spectroscopy*. Elsevier, Amsterdam, Second Edition 1985.
49. Voigt EM and Reid C: Ionization potentials of substituted benzenes and their charge-transfer spectra with tetracyanoethylene. *Journal of the American Chemical Society* 1964; 86: 3930-34.
50. Rathore R, Linderman SV and Kochi JK: Charge-transfer probes for molecular recognition via steric hindrance in donor-acceptor pairs. *Journal of the American Chemical Society* 1997; 119: 3393-04.
51. Briegleb G: Electron affinities of organic molecules. *Angewandte Chemie* 1964; 76: 326-41.
52. Aloisi GG and Pignataro S: Molecular complexes of substituted thiophens with σ and π acceptors. Charge transfer spectra and ionization potentials of the donors. *Journal of the Chemical Society, Faraday Transactions* 1973; 169: 534-39.
53. McConnel HM, Ham JJ and Platt JR: Regularities in the spectra of molecular complexes. *Journal of Chemical Physics* 1953; 21: 66-70.
54. Gaber M, El-Morsi MA and Abd-El-Ghafar M: Ionization-potentials and electro-affinities of organic molecules from electron charge-transfer spectra. *Journal of the Chemical Society of Pakistan* 1988; 10: 125-29.
55. Briegleb G and Czekalla J: Intensity of electron transition bands in electron donor-acceptor complexes. *Zeitschrift für Physikalische Chemie (Frankfurt)* 1960; 24: 37-54.
56. Person WP: Thermodynamic properties of donor-acceptor complexes. *Journal of the American Chemical Society* 1962; 84: 536-40.
57. International Conference on Harmonization of Technical Requirements for Registration of Pharmaceuticals for Human Use. ICH Harmonized Tripartite Guideline, Validation of Analytical Procedures: Text and Methodology, Q2(R1). Complementary Guideline on Methodology dated 06 November 1996, ICH, London 2005.
58. Miller JC and Miller JN: *Statistics for Analytical Chemistry*. England: Ellis Horwood Ltd., Second Edition 1988.
59. Irving HMNH, Freiser H and West TS: *IUPAC Compendium of Analytical Nomenclature Definitive Rules*. Oxford: Pergamon Press 1981.

How to cite this article:

Alghanmi RM and Alhazmi LY: Spectrophotometric determination of mebendazole through charge transfer interactions. *Int J Pharm Sci & Res* 2019; 10(5): 2504-15. doi: 10.13040/IJPSR.0975-8232.10(5).2504-15.

All © 2013 are reserved by International Journal of Pharmaceutical Sciences and Research. This Journal licensed under a Creative Commons Attribution-NonCommercial-ShareAlike 3.0 Unported License.

This article can be downloaded to **Android OS** based mobile. Scan QR Code using Code/Bar Scanner from your mobile. (Scanners are available on Google Play store)